Eur. Phys. J. Plus (2024) 139:330
https://doi.org/10.1140/epjp/s13360-024-05115-0

THE EUROPEAN PHYSICAL JOURNAL PLUS

Regular Article

Thyroid and contralateral breast surface dose variation in mammography: a phantom study on the role of breast tissue composition

Fatih Ekinci, Engin Aşlar[a]

Institute of Nuclear Sciences, Ankara University, Beşevler, 06100 Ankara, Türkiye

Received: 29 February 2024 / Accepted: 20 March 2024
© The Author(s) 2024

Abstract The organs of the thyroid and contralateral breast can be exposed to radiation because of scattered x-rays during mammography. It is important to determine the dose values of these quantities in terms of the risk of triggering a second cancer induction for both organs. In the present study, thyroid and contralateral breast surface doses were investigated with LiF:Mg,Ti (TLD-100) dosimeters for three types of BR-12 phantoms with glandularity/fat tissue ratios (70%/30%, 50%/50% and 30%/70%) over four views as in the real patient situation in Mo/Mo and Mo/Rh anode/filter combinations in each phantom thickness as opposed to a single glandular/fat tissue commonly used in the literature. Both thyroid and contralateral surface doses increased with increasing both phantom thickness and glandularity/fat ratio. The thyroid surface doses changed within 0.06–0.18 mGy and 0.05–0.14 mGy according to phantom thickness of 2 to 6 cm for the glandularity/adipose of 50%/50% in the Mo/Mo and Mo/Rh, respectively. On the other hand, the contralateral breast surface doses were within 0.35–1.39 mGy and 0.40–0.99 mGy for 50%/50% in the Mo/Mo and Mo/Rh, respectively. Based on a 70%/30% breast composition with a phantom thickness of 6 cm, the thyroid and contralateral breast surface doses increased by approximately 40% compared with 50%/50% for both Mo/Mo and Mo/Rh. These results showed that both thyroid and contralateral breast surface doses significantly depend on the glandularity/fat composition of the breast. Therefore, the outputs of this study may contribute to future studies aimed at reducing the doses received by organs during examination.

1 Introduction

Breast cancer is the most common cancer among women worldwide. Mammography is the most important technique widely used in the diagnosis of breast cancer [1]. The use of X-rays as ionizing radiation in mammography systems is a concern for patients before examination [2, 3]. During mammography, scattered x-rays may increase the risk of second cancer formation in organs such as the thyroid and contralateral breast [4, 5].

The organ doses for the contralateral breast, eye, heart, lung, and thymus were investigated using Monte Carlo simulations by Sechopoulos et al. [6]. The contralateral breast, eye, heart, lung, and thymus doses were 20.8, 2.2, 0.8, 0.7 and 0.7 μGy for respective organs. In the study performed by Baptista et al. [7], thyroid doses were investigated using a female voxel for 28 kVp in digital mammography (DM) and digital breast tomosynthesis (DBT). Thyroid surface doses were found at 273 μGy and 347 μGy, for DM and DBT, respectively. Chetlen et al. [8] measured the surface dose in organs such as the thyroid, salivary gland, and sternum in 207 patients with an average breast compression thickness of 62 mm. The surface doses of the left and right thyroid glands were 0.24 and 0.25 mGy, respectively. Chusin et al. [9] investigated the scatter dose in the eye and thyroid surface dose for breast tomosynthesis using randophantom for a breast thickness of 4.5 cm. The average thyroid surface dose for 4.5 cm was reported as 174.9 μGy.

On the other hand, radiation doses to the contralateral breast have been investigated in patients with mostly radiotherapy treatments [4, 10–16]. On the other hand, in mammography, Lee and Lee [17] reported an average contralateral breast surface dose of 0.66 mGy. According to this study, the dose absorbed by the contralateral breast made up ~ 45% of the dose directly delivered to the breast being imaged. Koo and Lee [18] studied various regions of the contralateral breast surface dose in terms of scattered radiation. The medial region of the breast received a dose of 5.88 mSv, whereas the other parts of the breast (upper, lower, nipple, etc.) received a dose range of 0.01–0.09 mSv.

Studies in the literature have mostly been conducted on phantoms with specific phantom thicknesses and glandular and fat tissue compositions. On the other hand, in a real situation, the thyroid and contralateral breast surface doses vary depending on the glandular/fat ratio composition and phantom thickness. Therefore, organ doses will differ according to the thickness of the phantom and glandular/fat ratios. The main innovation of this study is the evaluation of scattering doses for varying phantom thicknesses

[a] e-mail: easlar@ankara.edu.tr (corresponding author)

Published online: 15 April 2024

for three types of phantoms with glandularity/fat tissue ratios over four views, 2 craniocaudal (CC) and two mediolateral oblique (MLO) as in the real patient situation in Mo/Mo and Mo/Rh.

In this study, the variation in the thyroid and contralateral breast surface doses were evaluated using LiF:Mg,Ti (TLD-100) dosimeters according to three different BR-12 phantoms with glandularities of 70%/30%, 50%/50%, and 30%/70% at phantom thicknesses between 2 and 6 cm for Mo/Mo and Mo/Rh. Knowing the changes in dose values according to the glandular/fat ratio may provide important results in understanding the degree of variation in dose values in mammography. Additionally, the outputs of the study may be beneficial for future studies aimed at shielding the thyroid and contralateral breast organs.

2 Materials and methods

2.1 Materials

LiF:Mg,Ti dosimeters, purchased from the Harshaw Company in Ohio, USA and commercially known as TLD-100, were used in this study. Their dimensions are in the square form of $3.2 \times 3.2 \times 0.89$ mm. Measurements were performed using a Harshaw TLD-3500 Reader. The Alpha RT MGF-101 mammography device equipped with a constant molybdenum anode and two filters with molybdenum (Mo) and rhodium (Rh) of thicknesses of 30 and 25 μm, respectively, was used. Three types of BR-12 phantoms brand of CIRS with dimensions 12.5×10.0 cm^2 were used to simulate breast for different thicknesses between 2 and 6 cm. Their glandularity/fat tissue compositions were 30%/70%, 50%/50%, and 70%/30%. The female Anderson randophantom was used to determine the surface doses for the thyroid and contralateral breast organs. A 10X6-6 M Radcal ionization chamber with a flat energy response over the energy range of 10.0–40.0 keV was used for calibration of the dosimeters. The measurement positions of the dosimeters on the phantom were shown in Fig. 1a and b for both the thyroid and contralateral breast, respectively. Six dosimeters were placed in the thyroid area, three on the right and one on the left. For the measurement of the contralateral breast, a total of eight dosimeters were placed, four in each region: the inner left and the outer right. A total of four views (2 CC and 2 MLO) were included for thyroid surface dose measurements from the left and right breasts, whereas contralateral breast surface dose measurements included two views (1 CC and 1 MLO) obtained from a single breast.

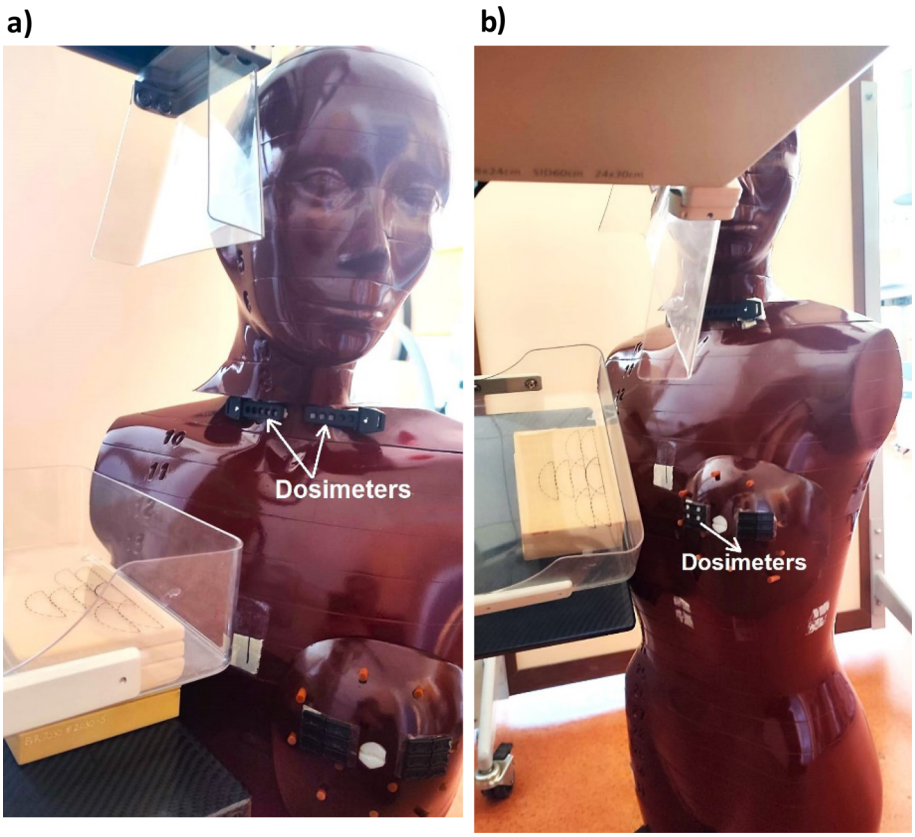


Fig. 1 Measurement positions of the dosimeters: **a** Thyroid surface region and **b** Contralateral breast surface region

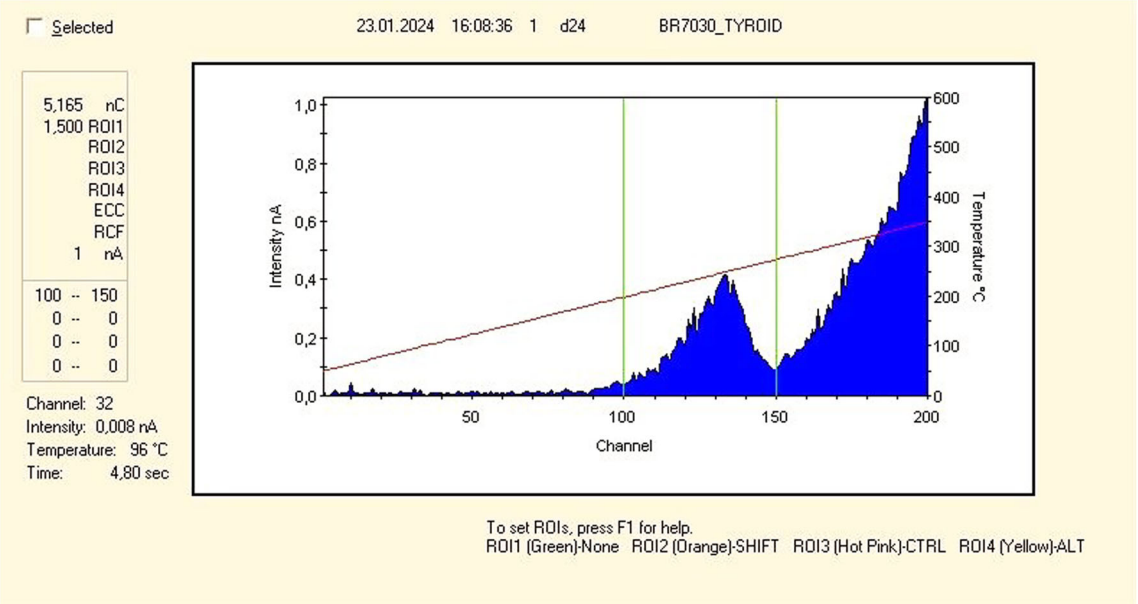


Fig. 2 The TL glow curve of TLD-100 obtained for thyroid surface dose for Mo/Mo situation

2.2 Methods

All irradiation in mammography was performed under semi-automatic exposure control (constant tube loading (kVp) and variable tube current (mAs)). Calibration of the dosimeters was performed at 28 kVp and 50 mAs for both Mo/Mo and Mo/Rh anode filter combinations. In total, 120 dosimeters with a standard deviation ~ 5% have been chosen for measurement. The element correction factors (ECC) which consider the intensity differences between the dosimeters were calculated using the following equation [19]:

$$\text{ECC} = \text{Mean intensity of TLD (nC)}/\text{Intensity of each TLD}$$

The reader calibration factor (RCF), which is the transition factor from reader intensity to dose values, was determined according to the formula [19]:

$$\text{RCF} = \text{Mean intensity of TLD (nC)}/\text{dose (mGy)}$$

Finally, dose values for the thyroid and contralateral breast organs were obtained as follows [19]:

$$\text{Dose} = \text{ECC} \times \text{Intensity of each TLD}/\text{RCF}$$

The obtaining of the calibration factors was the same as that in the studies of [20–22]. In our situation, RCF values were determined separately for Mo/Mo and Mo/Rh at 28 kVp and 50 mAs (corresponding air kerma of 6.45 mGy and 4.83 mGy for Mo/Mo and Mo/Rh, respectively). As a conclusion, RCF values were obtained at 5.87 mGy/nC and 5.41 mGy/nC for Mo/Mo and Mo/Rh, respectively. TL measurement was carried out by heating dosimeters up to 350 °C with a heating rate of 10 °C/s and measurement time of 30 s, after preheating them 100 °C for 10 min. By choosing a heating rate of 10 °C/s, which seems relatively high in the study, using ROI in dose measurements, and selecting the same heating rate throughout the measurement, a possible decrease in TL intensity due to thermal quenching and temperature lag was prevented [23]. The annealing of dosimeters was performed standardly 400 °C for 1 h and subsequently at 100 °C for 2 h in an oven. For the uncertainty in the entrance surface air kerma (ESAK) obtained according to the ionization chamber, the 4% value given in the calibration certificate was included [24]. The intensity value was determined as the mean area value of three dosimeters under regions of interest (ROI) by taking the region of the 100–150 channel, including three peaks in the glow curve of TLD-100 [25]. Figure 2 shows the TL glow curve of TLD-100 obtained for thyroid surface dose for Mo/Mo situation. Errors in the figures for thyroid and contralateral surface doses were calculated by considering the standard deviation of the dosimeters obtained from three dosimeters from the mean.

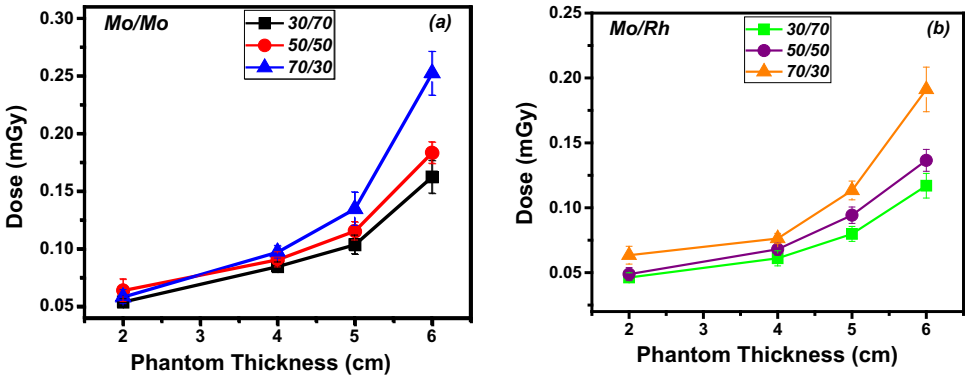


Fig. 3 Variation of thyroid surface dose according to different glandularity/fat compositions at different phantom thicknesses: **a** Mo/Mo; **b** Mo/Rh

Table 1 Relative difference (%) in thyroid surface dose for different glandularity/fat tissue ratios based on glandularity of 50%/50% for both Mo/Mo and Mo/Rh

Relative difference (%)	Mo/Mo		Mo/Rh	
Phantom thickness (cm)	(30%/70%)–(50%/50%)	(70%/30%)–(50%/50%)	(30%/70%)–(50%/50%)	(70%/30%)–(50%/50%)
2	− 15.50	− 8.82	− 5.37	29.82
4	− 6.54	7.28	− 6.88	12.17
5	− 11.99	18.67	− 13.72	20.40
6	− 11.44	37.55	− 14.31	36.49

3 Results and discussion

3.1 Thyroid surface dose results

Figure 3 shows the variation of thyroid surface dose obtained at different glandularity/fat compositions of 30%/70%, 50%/50%, and 70%/30% for Mo/Mo and Mo/Rh anode filter combinations.

For both anode filter combinations, the thyroid surface dose increased with increasing phantom thickness. Although it was not directly related to this study, this increase had a similar trend for the entrance surface dose (ESD) and mean glandular dose (MGD) increment with increasing phantom thickness [20, 21]. At the same time, thyroid surface doses increased as the glandularity/fat ratio increased. This is due to the increase in tube loading (mAs) along with the thickness of the phantom and the increase in glandularity/fat composition. In a study by Verma et al. [26], it was reported that thyroid surface doses increased as the phantom thickness increased from 2 to 5 cm. In our study, the increase in thyroid surface doses with increasing phantom thickness was compatible with that reported by Verma et al. [26]. On the other hand, no change was observed in terms of glandularity change at 2 cm. The main reason for this is that tube loading at 2 cm did not change much. In addition, the peaks were not observed in the glow curve.

According to Fig. 3a and b, the increase in the doses became more evident after 4 cm. The highest increase rate was observed at 6 cm. In conclusion, thyroid surface doses varied between 0.05 and 0.16 mGy for 30%/70%, 0.06–0.18 mGy for 50%/50%, and 0.06–0.25 mGy for 70%/30%, depending on phantom thicknesses of 2 and 6 cm for Mo/Mo. On the other hand, it changed between 0.05 and 0.12 mGy for 30%/70%, 0.05–0.14 mGy for 50%/50%, and 0.06–0.19 mGy for 70%/30% for Mo/Rh. When the thyroid surface dose values obtained in our study were compared with those reported by Sechopoulos et al. [6] and Sechopoulos and Hendrick [27], they were significantly higher than those reported. The reason for this discrepancy is considered that the doses measured in these studies were thyroid organ doses rather than thyroid surface doses. In addition, the number of views on the breast and the simulation method significantly changed the obtained values. On the other hand, thyroid surface doses were in good agreement with the values of 0.24–0.25 mGy for an average breast thickness of 6.2 cm given by Chetlen et al. [8] and the value of 0.17 mGy reported by Chusin et al. [9] for a phantom thickness of 4.5 cm. Furthermore, our results obtained for thyroid surface doses were consistent with those of Pyka et al. [5], Baptista et al. [7], Whelan et al. [28], Kunosic et al. [29], and Pirchio et al. [30]. Another observation related Fig. 3a and b is that the thyroid surface dose obtained in Mo/Mo was larger than that obtained for Mo/Rh for each glandularity/fat ratio. The dose value obtained for Mo/Mo was approximately 30% higher than that for Mo/Rh.

Table 1 presents the relative difference in thyroid surface dose according to different glandularity/fat ratios on the basis of 50%/50% for both Mo/Mo and Mo/Rh. In Table 1, the negative values seen in the first and second columns for Mo/Mo and Mo/Rh indicate that the thyroid surface doses obtained for 30%/70% were higher than those obtained for 50%/50%, contrary to expectations.

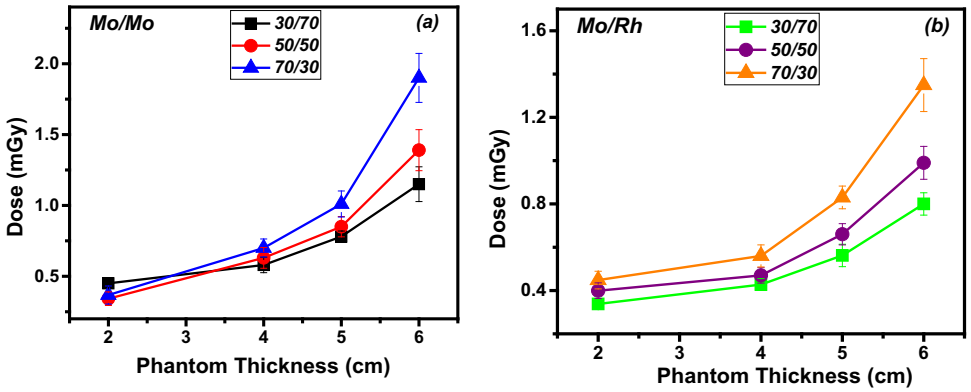


Fig. 4 Variation of contralateral breast surface dose according to different glandularity/fat compositions at different phantom thicknesses: **a** Mo/Mo; **b** Mo/Rh

Table 2 Relative difference (%) in contralateral breast surface dose for different glandularity/fat tissue ratios based on the glandularity/fat ratio of 50%/50% for both Mo/Mo and Mo/Rh

Relative difference (%)	Mo/Mo		Mo/Rh	
Phantom thickness (cm)	(30%/70%)–(50%/50%)	(70%/30%)–(50%/50%)	(30%/70%)–(50%/50%)	(70%/30%)–(50%/50%)
2	31.70	7.59	− 15.36	12.27
4	− 7.94	11.11	− 9.00	19.15
5	− 8.24	17.65	− 16.67	25.76
6	− 17.27	36.69	− 19.18	36.28

As the glandularity ratio increased, the increase in the relative difference (%) for the situation of (70%/30%)–(50%/50%) became greater for both anode filter combinations. For example, at a phantom thickness of 6 cm, the thyroid surface dose increased by nearly 40% compared with the value obtained for 50%/50%. This result clearly demonstrates the importance of the glandularity effect on the thyroid surface dose.

3.2 Contralateral breast surface dose results

Fig. 4 shows the variation of contralateral breast surface dose for different glandularity/fat compositions, 30%/70%, 50%/50%, and 70%/30% for Mo/Mo and Mo/Rh with different phantom thicknesses. These results represent the surface doses obtained from dosimeters on the left inner side of the breast. On the other hand, the surface doses obtained from dosimeters placed on the outer surface of the breast did not vary according to phantom thickness and glandularity, possibly because the dosimeters were located far away from the irradiation area. According to Fig. 4a and b, the contralateral breast surface dose showed a regular increase with increasing phantom thickness and glandularity ratio, similar to the thyroid surface dose. They varied between 0.45 and 1.15 mGy 30%/70%, 0.35–1.39 mGy for 50%/50%, and 0.37–1.90 mGy for 70%/30%, depending on phantom thicknesses of 2 and 6 cm for Mo/Mo. For Mo/Rh, doses varied from 0.34 to 0.80 mGy for 30%/70%, 0.40–0.99 mGy for 50%/50%, and 0.45–1.35 mGy for 70%/30%, depending on phantom thicknesses of 2 and 6 cm.

When the contralateral breast dose obtained in the case of 6 cm Mo/Mo and Mo/Rh with 50%/50% was compared with the thyroid surface dose, the contralateral breast dose was nearly six times higher than the thyroid surface dose for both Mo/Mo and Mo/Rh. This result indicates that the contralateral breast surface dose was exposed to a significantly higher dose than the thyroid surface dose. In the study conducted by Judge et al. [31], it was emphasized that scattering should not be ignored, especially in the forward direction in mammography, just as scattering effects were important in ion therapy [32, 33]. According to Sechopoulos et al. [6], the contralateral breast surface dose was reported 95.8 μGy for Mo/Mo at 30 kVp. This value was very low compared with the results of our studies. This may be because in the study by Sechopoulos et al. [6], they performed a study over two views and it was done directly with the Monte Carlo simulation program without an experimental study. The contralateral dose surface values obtained in our study were higher than the 0.66 mGy contralateral surface dose given by Lee and Lee [17], whereas they were lower than the contralateral dose value reported by Koo and Lee [18]. As mentioned above, the differences in the doses depend not only on the equipment used and the number of views of the breast but also significantly on the measurement position. In conclusion, the contralateral breast surface was exposed to a significantly higher amount of radiation during the examination. Table 2 presents the relative difference in the contralateral breast surface dose based on the glandularity/fat ratio of 50%/50% for Mo/Mo and Mo/Rh anode filter combinations.

Similar to the thyroid surface dose, the contralateral breast surface dose obtained in 30%/70% was lower than that obtained in 50%/50% for both Mo/Mo and Mo/Rh. Therefore, in Table 1, the first columns have a negative value. As an exception, a positive

value was obtained at 2 cm for Mo/Mo. On the other hand, in the case of difference (70%/30%)–(50%/50%), the variation in contralateral breast surface dose was greatest. In this case, an approximately 40% increase in the 6 cm phantom thickness was observed for both anode filter combinations. In other words, contralateral breast surface doses increased significantly because of scattered x-rays, especially for thick and dense breasts, similar to the thyroid surface dose.

4 Conclusion

In this study, the variation in the thyroid and contralateral breast surface doses was investigated with LiF:Mg,Ti (TLD-100) dosimeters for three types of BR-12 phantoms with glandularity/fat tissue ratios (70%/30%, 50%/50% and 30%/70%) in Mo/Mo and Mo/Rh for each phantom thickness. Both thyroid and contralateral surface doses increased with increasing both phantom thickness and glandularity/fat ratio. The thyroid surface doses changed within mGy and 0.05–0.14 mGy according to phantom thickness of 2 to 6 cm for 50%/50% in the Mo/Mo and Mo/Rh, respectively. On the other hand, the contralateral breast surface doses were within 0.35–1.39 mGy and 0.40–0.99 mGy for 50%/50% in the Mo/Mo and Mo/Rh situations, respectively. At a phantom thickness of 6 cm, thyroid and contralateral breast surface doses obtained in the 70%/30% increased by ~40% for both Mo/Mo and Mo/Rh compared with 50%/50%. According to these results, both thyroid and contralateral breast surface doses significantly depend on both glandularity/fat composition of the breast and phantom thickness. Therefore, the outputs of this study may contribute to future studies aimed at reducing the doses received by organs during examination.

Funding Open access funding provided by the Scientific and Technological Research Council of Türkiye (TÜBİTAK).

Data availability This manuscript has associated data in a data repository. [Authors' comment: The data that support the findings of this study are available from the corresponding author upon reasonable request].

Declarations

Conflict of interest None.

Ethical approval There are no human subjects in this article, and informed consent is not applicable.

Open Access This article is licensed under a Creative Commons Attribution 4.0 International License, which permits use, sharing, adaptation, distribution and reproduction in any medium or format, as long as you give appropriate credit to the original author(s) and the source, provide a link to the Creative Commons licence, and indicate if changes were made. The images or other third party material in this article are included in the article's Creative Commons licence, unless indicated otherwise in a credit line to the material. If material is not included in the article's Creative Commons licence and your intended use is not permitted by statutory regulation or exceeds the permitted use, you will need to obtain permission directly from the copyright holder. To view a copy of this licence, visit http://creativecommons.org/licenses/by/4.0/.

References

1. National Cancer Institute, 2024. https://www.cancer.gov/types/breast/hp/breast-screening-pdq. Accessed 20 Feb 2024
2. M. Singh, B. Jangra, Association between body mass index and risk of breast cancer among females of north India. South Asian J. Cancer **2**(3), 121 (2013)
3. L. Wilkinson, T. Gathani, Understanding breast cancer as a global health concern. Br. J. Radiol. **95**(1130), 20211033 (2022)
4. B.A. Fraass, P.L. Roberson, A.S. Lichter, Dose to the contralateral breast due to primary breast irradiation. Int. J. Radiat. Oncol. Biol. Phys. **11**(3), 485–497 (1985)
5. M. Pyka, P. Eschle, C. Sommer, M.S. Weyland, R. Kubik, S. Scheidegger, Effect of thyroid shielding during mammography: measurements on phantom and patient as well as estimation with Monte Carlo simulation. Eur. Radiol. Exp. **2**(1), 1–10 (2018)
6. I. Sechopoulos, S. Suryanarayanan, S. Vedantham, C.J. D'Orsi, A. Karellas, Radiation dose to organs and tissues from mammography: Monte Carlo and phantom study. Radiology **246**(2), 434–443 (2008)
7. M. Baptista, S. Di Maria, S. Barros, C. Figueira, M. Sarmento, L. Orvalho, P. Vaz, Dosimetric characterization and organ dose assessment in digital breast tomosynthesis: measurements and Monte Carlo simulations using voxel phantoms. Med. Phys. **42**(7), 3788–3800 (2015)
8. A.L. Chetlen, K.L. Brown, S.H. King, C.J. Kasales, S.E. Schetter, J.A. Mack, J. Zhu, Scatter radiation dose from digital screening mammography measured in a representative patient population. Am. J. Roentgenol. **206**(2), 359–64 (2016)
9. T. Chusin, K. Matsubara, A. Takemura, R. Okubo, Y. Ogawa, Assessment of scatter radiation dose and absorbed doses in eye lens and thyroid gland during digital breast tomosynthesis. J. Appl. Clin. Med. Phys. **20**(1), 340–347 (2019)
10. R. Muller-Runkel, U.P. Kalokhe, Scatter dose from tangential breast irradiation to the uninvolved breast. Radiology **175**(3), 873–876 (1990)
11. N. Jamal, K.R. Das, Measurement of dose to the contralateral breast during radiation therapy for breast cancer: reduction by the use of superflab. Australas. Phys. Eng. Sci. Med. **24**, 102–105 (2001)
12. N. De La Torre, C.T. Figueroa, K. Martinez, S. Riley, J. Chapman, A comparative study of surface dose and dose distribution for intact breast following irradiation with field-in-field technique vs the use of conventional wedges. Med. Dosim. **29**(2), 109–114 (2004)
13. B.S. Yadav, S.C. Sharma, F.D. Patel, S. Ghoshal, R.K. Kapoor, Second primary in the contralateral breast after treatment of breast cancer. Radiother. Oncol. **86**(2), 171–176 (2008)
14. M. Tolia, K. Platoni, A. Foteineas, M.A. Kalogeridi, A. Zygogianni, N. Tsoukalas, V. Kouloulias, Assessment of contralateral mammary gland dose in the treatment of breast cancer using accelerated hypofractionated radiotherapy. World J. Radiol. **3**(9), 233 (2011)

15. S.A. Rather, M.M.U. Haq, N.A. Khan, A.A. Khan, A.G. Sofi, Determining the contralateral breast dose during radiotherapy of breast cancer using rainbow dosimeter. J. Radiat. Res. Appl. Sci. **7**(4), 384–389 (2014)
16. P. Ramachandran, A. Smith, J. Hagekyriakou, J. Hughes, P. Lonski, B. Howard, T. Kron, Contralateral breast dose with electronic compensators and conventional tangential fields–a clinical dosimetric study. Z. Med. Phys. **31**(4), 347–354 (2021)
17. D.Y. Lee, J.S. Lee, Designing a shield to reduce radiation dose during mammography: dosimetric evaluation. Int. J. Radiat. Res. **17**(1), 127–135 (2019)
18. B.Y. Koo, K.S. Lee, Reduction of scattered radiation dose by X-ray shielding during mammography. Radiat. Phys. Chem. **177**, 109111 (2020)
19. Thermo Electron Corporation, *Model 3500 manual TLD reader with WinREMS* (Thermo Electron Corporation Radiation Measurement and Protection, Oakwood Village, OH, 2005)
20. E. Aşlar, E. Şahiner, G.S. Polymeris, N. Meriç, Feasibility of determining entrance surface dose (ESD) and mean glandular dose (MGD) using OSL signal from BeO dosimeters in mammography. Radiat. Phys. Chem. **177**, 109151 (2020)
21. E. Aşlar, Characterization of CaF2: Dy (TLD-200) dosimeters and determination of dosimetric quantities in mammography. Radiat. Meas. **154**, 106779 (2022)
22. V.E. Kafadar, Ö. Yegen, ŞB. Çifci, İ Karslıoğlu, Outfield radiation dose determination by TLD-100 in the treatment of breast cancer using hypofractionated radiation therapy. Eur. Phys. J. Plus **138**(10), 922 (2023)
23. E. Aşlar, Investigation of thermal quenching effect for lithium fluoride (LiF) Type dosimeters. Cumhur. Sci. J. **44**(2), 389–395 (2023)
24. Radcal, 2006. Available from: https://radcal.com/rdclwp/wp-content/uploads/2016/10/radcal-10X6-6M-chamber-spec-sheet.pdf. Accessed 10 Feb 2024
25. E. Aşlar, A photo-transfer thermoluminescence (PTTL) study of TLD-100 over a wide dose range. Süleyman Demirel Univ. Fac. Arts Sci. J. Sci. **18**(3), 268–275 (2023)
26. R. Verma, G.K. Jain, A. Chougule, Evaluation and analysis of entrance surface air kerma of the thyroid gland during breast cancer screening mammography. Radiat. Med. Prot. **2**(02), 67–71 (2021)
27. I. Sechopoulos, R.E. Hendrick, Mammography and the risk of thyroid cancer. Am. J. Roentgenol. **198**(3), 705–707 (2012)
28. C. Whelan, D. McLean, A. Poulos, Investigation of thyroid dose due to mammography. Australas. Radiol. **43**(3), 307–310 (1999)
29. S. Kunosic, D. Ceke, A. Beganovic et al., Effects of dispersed radiation on the thyroid and the gonads during mammography. HealthMED **5**(6), 1774–1781 (2011)
30. R. Pirchio, A. Stefanic, R.R. Rojas, Characterisation of TLDS-200 and OSLDS at low X-ray energies and determination of eye lens dose, thyroid dose and mean glandular dose during standard mammography and tomosynthesis. Radiat. Prot. Dosim. **186**(4), 469–478 (2019)
31. M.A. Judge, E. Keavey, N. Phelan, Scatter radiation intensities around full-field digital mammography units. Br. J. Radiol. **86**(1021), 20120130–20120130 (2013)
32. F. Ekinci, E. Bostancı, S.M. Güzel, Ö. Dağlı, Analysing the effect of a cranium thickness on a Bragg peak range in the proton therapy: a TRIM and GEANT4 based study. St Petersb. Polytech. Univ. J. Phys. Math. **15**(2), 64–78 (2022)
33. F. Ekinci, Investigation of tissue equivalence of phantom biomaterials in 4He heavy ion therapy. Radiat. Eff. Defects Solids **178**(3–4), 500–509 (2023)